Chemical
Science

Accepted Manuscript

This article can be cited before page numbers have been issued, to do this please use: D. J. van Dijken, P. Stacko, M. C.A. Stuart, W. Browne and B. L. Feringa, *Chem. Sci.*, 2016, DOI: 10.1039/C6SC02935C.

ROYAL SOCIETY
OF CHEMISTRY

rsc.li/chemical-science

View Article Online
DOI: 10.1039/C6SC02935C

Journal Name

ARTICLE

Chirality Controlled Responsive Self-Assembled Nanotubes in Water

Received 00th January 20xx,
Accepted 00th January 20xx

DOI: 10.1039/x0xx00000x

www.rsc.org/

D. J. van Dijken,[†,a] P. Štacko,[†,a] M. C. A. Stuart,[a,b] W. R. Browne[a] and B. L. Feringa*[,a]

The concept of using chirality to dictate dimensions and store chiral information in self-assembled nanotubes in a fully controlled manner is presented. We report a photoresponsive amphiphile that co-assembles with its chiral counterpart to form nanotubes and demonstrate how chirality can be used to effect the formation of either micrometer long, achiral nanotubes or shorter (~ 300 nm) chiral nanotubes that are bundled. The nature of these assemblies is studied using a variety of spectroscopic and microscopic techniques and it is shown that the tubes can be disassembled with light, thereby allowing the chiral information to be erased.

Introduction

A fascinating aspect and crucial feature of complex, multifunctional self-assembled objects found in Nature is that they are dynamic, allowing a multitude of biological processes to rely on feedback-controlled communication.[1] In other words, the self-assembled structure can adopt in response to an input signal. This ability to adjust in response to stimuli is crucial for correct functioning of many bioprocesses.[2] Therefore, the design and synthesis of artificial systems that can respond to external stimuli is highly warranted in order to better understand and mimic highly sophisticated natural systems. Furthermore, such systems potentially provide a basis for novel smart materials and nanoscale devices, for example for sensing and drug delivery.[3]

The use of chirality to control or initiate self-assembly offers a particularly interesting approach, as the living world around us is made up of chiral molecules of a unique handedness. Many natural systems, such as for example enzymes, are extremely effective in discriminating enantiomers and in the assembly of biomaterials like proteins and DNA, stereochemistry is key with a delicate interplay of molecular and supramolecular chirality.[4] Amplification of chirality is necessary for the emergence of homochirality from a pool of nearly racemic compound and is thought to be essential in the origin of life and the emergence of biomaterials and bionanosystems.[5] In recent years, amplification of chirality has been exploited in the field of supramolecular chemistry and this principle has been applied in supramolecular polymers,[6] gels,[7] organic nanotubes,[8] liquid crystals[9] and other assemblies.[10] The groups of Aida and Meijer in parallel pioneered the possibility to amplify chirality in supramolecular systems, exploring the "majority rules" principle,[8c,11] where the major enantiomer determines the chirality of the entire assembly. In addition, the "sergeant-soldier" principle has been reported for transfer of chirality from monomers to supramolecular aggregates.[12–14] In the sergeant-soldier principle, as introduced by Green and coworkers,[15] a minor amount of the chiral compound (sergeant), used as dopant, dictates the overall chirality of a system that is made up of mainly achiral material (soldiers).

In natural phospholipids, the most abundant constituent of cell membranes, the chiral information is often present in the aliphatic tails and the specific chiral information in these phospholipid backbones, present on the internal hydrophobic side of the self-assembled phospholipid bilayer, is of major importance.[16] It is therefore remarkable that in most artificial systems, to the best of our knowledge,[8c,11–14,17] the chiral information is introduced in the part of the molecules that are not involved in the main binding interactions that lead to assembly into a larger aggregate. Often, changes in this hydrophobic part of the self-assembling molecules distorts their packing to such an extent that well-defined supramolecular structures are no longer obtained.

Results and Discussion

Design

Inspired by Nature, the present study focuses on the use of chirality as a tool to govern defining parameters in complex supramolecular assemblies and we show that through molecular design, properties of the well-defined aggregates as a whole, such as dimensions, aggregation, overall chirality and photoresponsiveness, can be controlled. Previously, a light-

---

[a] *Centre for Systems Chemistry, Stratingh Institute for Chemistry, University of Groningen, Nijenborgh 4, 9747 AG, Groningen, The Netherlands*
[b] *Groningen Biomolecular Sciences and Biotechnology Institute, University of Groningen, Nijenborgh 7, 9747 AG, Groningen, The Netherlands*

† These authors contributed equally.

Electronic Supplementary Information (ESI) available: [Detailed experimental procedures and analyses, UV-vis absorption and CD spectroscopy, cryo-TEM and widefield microscopy]. See DOI: 10.1039/x0xx00000x

View Article Online
DOI: 10.1039/C6SC02935C

responsive, self-assembled nanotube system based on a photochemically active amphiphile **1** has been developed (Figure 1).[18] We envisioned that amplification of chirality may be possible in such rigid supramolecular nanotubes by doping achiral amphiphile **1** with small amounts of a closely related chiral analogue and that we can use this stereochemical feature as a distinct control element for self-assembled nanotubes. Toward this goal, chiral **2** was designed, which bears two stereocenters in the hydrophobic part of the amphiphile. The structure of amphiphiles **1** and **2** contains a photosensitive overcrowded alkene unit that links two hydrophilic oligo-ethylene glycol headgroups with two hydrophobic alkyl tails. The bis-thioxanthylidene core provides a photoreactive and fluorescent functionality,[19] and the oligo-ethylene glycol units facilitate solubility in water. The hydrophobic alkyl chains are positioned at the core structure to maximise interaction and facilitate supramolecular assembly by interdigitating upon aggregation to form a very robust bilayer, resulting in the formation of nanotubular assemblies.[18]

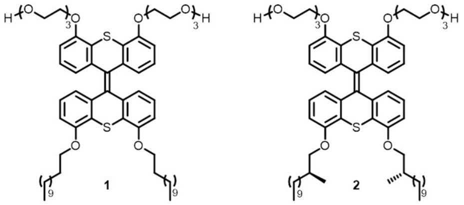

Figure 1. Design and structure of amphiphiles **1** (achiral) and **2** (chiral).

Here we show how chirality and morphology of self-assembled supramolecular nanotubes is controlled by changing the molar fraction of chiral constituent in the co-assembled nanotubes. The well-defined nanotubes have different diameters and show different behaviour depending on the ratio of chiral to achiral amphiphile building blocks. The chiral information, displayed by the nanotubes, can be erased with light *via* disassembly of the nanotubes. The nanotube systems presented here have several distinct differences compared to a number of supramolecular materials reported to date.[6–10] The nanotubes are remarkably rigid, self-assemble in water and are photoresponsive, which means that they can be disassembled with light.[18] Furthermore, the fact that our nanotubes form in water gives future opportunities for biocompatibility.

As the hydrophobic half of the molecule makes up the internal part of the bilayer after self-assembly, and is most probably densely packed,[18] we envisioned that the largest effect on the overall chirality could be obtained by introducing chirality in the hydrophobic alkyl chains. We furthermore reasoned that the packing of the molecules upon self-assembly would be least disturbed if the chirality is installed close to the aromatic core of the amphiphile. Two methyl groups were therefore introduced in amphiphile **2** at the C2 position of the alkyl chains (Figure 1) to generate single enantiomers with the stereogenic information.

Synthesis

A major challenge is the synthesis of both **1** and **2** in sufficient amounts to conduct the sergeant-soldier experiments. The synthesis of both amphiphiles is lengthy and contains some difficult steps. In this work, an efficient synthesis route for **1** and the chiral analogue **2** was developed (Schemes 1–2, see also Supporting Information).

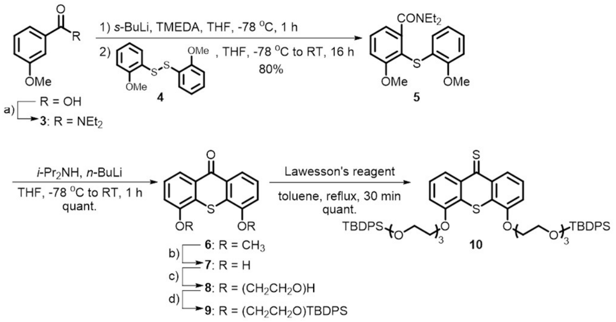

Scheme 1. Synthesis of hydrophilic precursor thioketone **10**. Reagents and conditions: (a) (1) $SOCl_2$ (2.4 equiv), CH_2Cl_2, reflux, 1 h; (2) Et_2NH (4.0 equiv), 0 °C to RT, 2 h, 98%; (b) BBr_3 (5.0 equiv), CH_2Cl_2, 0 °C to RT, 16 h, quant; (c) $TsO(CH_2CH_2O)_3H$ (2.0 equiv), Cs_2CO_3 (5.0 equiv), DMF, 110 °C, 16 h, 85%; (d) TBDPSCl (2.5 equiv), imidazole (3.3 equiv), CH_2Cl_2, 0 °C to RT, 1 h, 75%.

Selective functionalisation of (thio)xanthones in the desired 4- and 5-positions is not a trivial task and the key building block **7** was therefore prepared using a bottom-up approach. 3-Methoxybenzoic acid was transformed into its acid chloride and quenched with diethylamine to give amide **3** in excellent yield. Oxidation of 2-methoxybenzenethiol yields disulfide **2**, which was added to **3** after selective *ortho*-lithiation with *s*-BuLi and TMEDA at -78 °C to give thioxanthone precursor **5**. Regioselective lithiation using freshly prepared lithium diisopropylamine resulted in ring-closure to form **6**, which was subsequently deprotected with BBr_3 to give dihydroxy building block **7** in an overal yield of 78% over four linear steps. Hydrophilic ethylene glycol chains were introduced by deprotonation of the hydroxy moieties with Cs_2CO_3 and addition of an equimolar amount of mono-tosyl ethylene glycol. The terminal glycol groups of **8** were protected with TBDPS-groups and **9** was subsequently converted to its thioketone derivative **10**.

Hydrophobic chains were introduced by deprotonation of the hydroxy functionalities of **7** (Scheme 3) and addition of either dodecyl bromide or the chiral analogue **19** that was prepared using Evans methodology in analogy to the literature procedures.[20–23] Only one diastereomer of the latest reported intermediate was observed (see Supporting Information for details) and it was therefore concluded that the bromide **19** is enantiomerically pure. Compounds **11** and **20** were converted to their thioketone analogues in order to increase their reactivity and subsequently converted to hydrazones **13** and **21**, respectively, using hydrazine monohydrate at room temperature. The Barton-Kellogg reaction is routinely used for

View Article Online
DOI: 10.1039/C6SC02935C

the construction of highly demanding tetra-substituted double bonds, but commonly suffers from low yields. The original synthesis of the amphiphile was considerably improved by employing a mild oxidation of the hydrazones using MnO_2 at 0 °C and subsequent addition of thioketone **10** yielded episulfides **14** and **22** in 90% yield. The desulfurisation of the episulfides was achieved with PPh_3 and deprotection of the hydroxyl moieties with TBAF yielded achiral amphiphile **1** and its chiral analogue **2** in 45% and 35% overall yield for the longest linear sequences (10 steps).

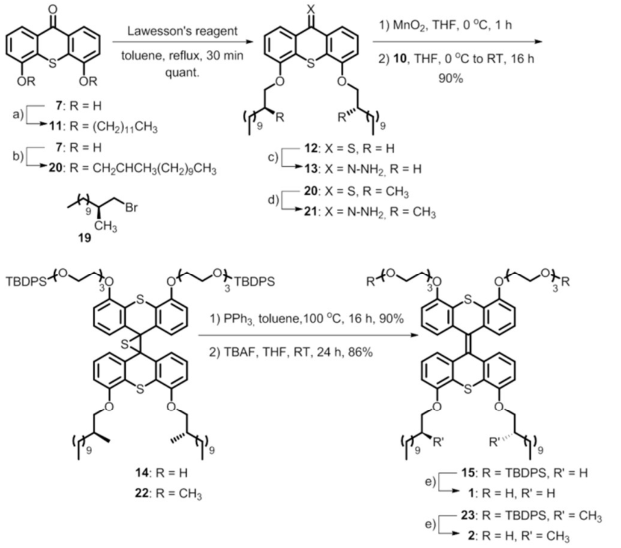

Scheme 2. Synthesis of achiral amphiphile **1** and chiral analogue **2**. Reagents and conditions: (a) $CH_3(CH_2)_{11}Br$ (2.6 equiv), Cs_2CO_3 (5.0 equiv), DMF, 110 °C, 16 h, 90%; (b) **19** (2.6 equiv), K_2CO_3 (5.0 equiv), DMF, 100 °C, 24 h, 91%; (c) $NH_2NH_2{\cdot}H_2O$ (39 equiv), THF, RT, 10 min, quant; (d) (1) Lawesson's reagent (1.5 equiv), toluene, reflux, 2 h; (2) $NH_2NH_2{\cdot}H_2O$ (19 equiv), THF, RT, 10 min, 83%; (e) TBAF (2.8 equiv), THF, 0 °C to RT, 24 h, 86–90%.

Self-Assembly

With achiral **1** and enantiopure **2** in hand, aggregation was first confirmed by cryo-TEM measurements. Amphiphile **1** self-assembles into micrometre long nanotubes (Figure 2a) when co-assembled with 1,2-dioleoyl-sn-glycero-3-phosphocholine (DOPC) 1:1.[18] Much to our delight, starting from a 1:1 mixture of **2** and DOPC, the formation of nanotubes from the chiral amphiphile was also observed (Figure 2b). Henceforth, assembly experiments were always conducted with amphiphile and DOPC in a ratio of 1:1 to the total amphiphile concentration. The nanotubes of **2** resemble the structures formed by amphiphile **1**.

The bilayers, making up the nanotube walls, were found to be 3 nm thick for both the tubes of pure achiral **1** and the homochiral amphiphile **2** and differences in bilayers were not observed by cryo-TEM. No other types of aggregates were found for either **1** or **2**. Furthermore, nanotubes of **1** are generally very straight and virtually no bends or turns were observed in the nanotubes. Although we observed that for nanotubes of **2** a higher amount of bent tubes was formed, compared to tubes of **1**, nanotubes of **2** showed in general linear structures that were uniform in nature. A distinct difference between nanotubes of pure achiral **1** and chiral **2** is that nanotubes of **1** (Figure 2a) are typically longer than a micrometre, while tubes of **2** (Figure 2b) are shorter; typically only ~300 nm long.

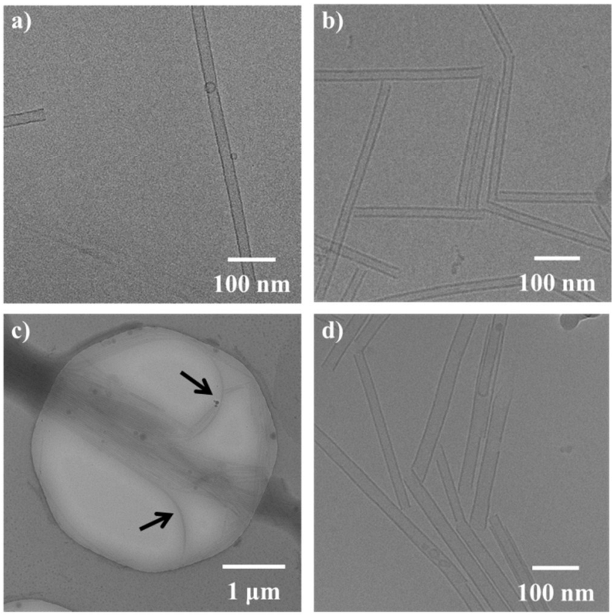

Figure 2. Cryo-TEM microscopy images of self-assembled nanotubes in water at a total concentration of 1 mg/mL. a) Nanotubes of achiral **1** with DOPC (1:1). b) Nanotubes of chiral **2** with DOPC (1:1). c) Nanotubes of **1** and **2** with DOPC (0.6:0.4:1). Arrows indicate nanotubes bending away from the "bundle". d) Nanotubes of **1** and **2** with DOPC (0.4:0.6:1).

In addition, we found that tubes of **2** tend to pack together more extensively (tube aggregation) than those of **1** at the same concentration, as observed by cryo-TEM. Figure 2b–c for example, shows a type of network in which several nanotubes align and pack together to form "bundles" for high content of (or exclusively) **2**. Nanotubes of achiral **1** are typically isolated and we found no evidence that they align with one another to a significant extent. While the reduced length of the nanotubes of **2** may be explained by a difference in packing due to the presence of the two methyl moieties in the interacting hydrophobic tails (increase in hydrophobic volume), we do not currently know why the shorter tubes tend to bundle together. Nanotubes of both **1** and **2** capped with DOPC vesicles were also found as reported for **1** previously,[18] and the tubes are not different in this regard. After confirming that both enantiopure amphiphile **2** and achiral amphiphile **1** form nanotubes, we set out to perform sergeant-soldier experiments by mixing varying ratios of **1** and **2**. In the mixed nanotubes (Figure 2c–d), nanotube formation was not inhibited at any ratio of amphiphiles **1**:**2**. Increasing the fraction of chiral **2** to over 50% (Figure 2d compared to 2c) results in tubes that are shorter than nanotubes of pure achiral **1**, typically ~ 300 nm in length, and more bundled, reminiscent of the tubes of pure **2** (Figure 2b). It should be noted that while in all samples both long and short tubes could be

View Article Online
DOI: 10.1039/C6SC02935C

observed, below 50% of **2**, the long tubes are far more abundant while mainly short tubes are present in the mixtures containing over 50% chiral **2**. Another observation is that the tubes of mixed amphiphiles bend more, as can be seen in Figure 2c (nanotubes are bending away from the "bundle" as indicated with black arrows).

Spectroscopic Studies

After having confirmed that nanotubes could be formed at different ratios of **1** and **2**, the spectroscopic properties were studied (Figure 3).

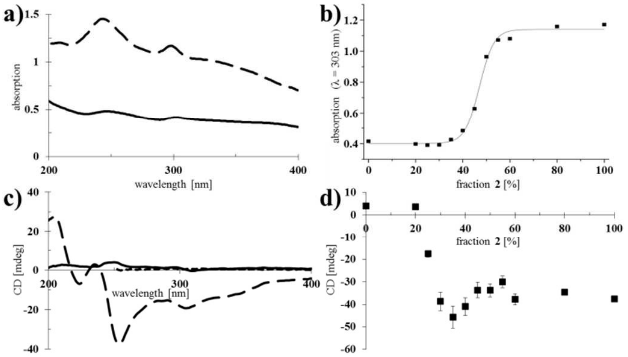

Figure 3. UV-vis absorption and CD spectra of nanotubes of **1** and **2**. a) UV-vis absorption spectra of assemblies of pure **1** (solid line, $1.6{\cdot}10^{-4}$ M in water) and pure **2** (dashed line, $1.6{\cdot}10^{-4}$ M in water). b) Absorption at λ = 303 nm as a function of the fraction of **2** in co-assembled nanotubes of **1** and **2** (data was fitted to sigmoidal curve using Origin software). c) CD spectra of nanotubes of **1** (solid line, $1.6{\cdot}10^{-4}$ M in water) and **2** (dashed line, $1.6{\cdot}10^{-4}$ M in water) and a solution of **2** (dotted line, $2.5{\cdot}10^{-5}$ M in $CHCl_3$; cut-off for $CHCl_3$ is λ = 260 nm). b) CD maximum at λ = 303 nm as a function of the fraction **2** in co-assembled nanotubes of **1** and **2**. Measurements were performed in triplo and error bars are shown.

Larger aggregates scatter more light and consequently, the baseline in absorption spectra increases.[24] Self-assembled samples of pure chiral **2** show more scattering than those of pure achiral **1** (Figure 3a), indicating the formation of the relatively large bundles of nanotubes, consistent with the observations by cryo-TEM (Figure 2). Mixed nanotubes that are composed of < 50% the chiral amphiphile **2** show similar absorption spectra as pure **1** (see Supporting Information for all UV-vis absorption spectra). Plotting the absorption (λ = 303 nm) as a function of the fraction of chiral amphiphile **2** in the mixed nanotubes, reveals a significant increase in scattering when the fraction of **2** exceeds 40%, with an undulation point at 47% (calculated by fitting a sigmoidal curve in Origin software; Figure 3b). Interestingly, the absorption remains nearly unchanged when increasing the fraction of chiral **2** from 50% to 100% (Figure 3b), which leads us to propose that a homogeneous population of bundled, shorter nanotubes is formed when chiral **2** is the major component, while the formation of longer, isolated nanotubes is favoured when the tubes mainly consist of achiral **1**. This is in agreement with the observation of more bundled, shorter nanotubes for the same samples, as measured by cryo-TEM (Figure 2).

We next set out to probe the induction of chirality based on the sergeant-soldier principle.[12–14, 17] We found that a solution of **2** in $CHCl_3$ is CD silent (Figure 3c, dotted line), likely because the chromophore is remote from, or not influenced by, the presence of the stereogenic centres. This offers good prospects for the concept of reading and erasing chiral information in the supramolecular assembly.[10a,25] Nanotubes of achiral **1** are also CD silent, as expected (Figure 3c, solid line). On the other hand, CD spectroscopy shows that nanotubes of chiral amphiphile **2** in water, exhibit Cotton effects with negative maxima at λ = 303, 256 and 225 nm and a positive maximum at λ = 208 nm (Figure 3c, dashed line). Subsequently, sergeant-soldier experiments were performed to investigate if a small fraction of chiral **2** is able to induce chirality in the otherwise achiral nanotubes of **1**. Starting at 25% of **2** in the co-assembled aggregates, the mixed nanotubes are indeed chiral as shown by plotting the CD maximum (303 nm) as function of the fraction of **2** (Figure 3d). Nanotubes with less than 25% of **2**, however, do not show any CD signal and plotting the CD maximum (λ = 303 nm) as a function of the fraction of chiral component **2** (Figure 3d), reveals a similar relation as between the absorption and the fraction of **2** (Figure 3b). In contrast to the Uv-vis absorption, which shows a sigmoidal relation with a sharp increase at 40% of **2**, however, the CD signal increases when the fraction of chiral compound **2** exceeds 25% and reaches a maximum at 35%, after which it decreases and reaches a constant value. Above a fraction of 50% of **2**, the nanotubes appear to be homogeneous and no differences could be observed for tubes that consist of 50–100% of the chiral amphiphile **2** (Figure 3d). Figure 4 shows a schematic model for the observed behaviour and properties of nanotubes consisting of achiral **1** and chiral **2** (with DOPC in a ratio of 1:1 amphiphile:DOPC) as a function of the fraction of **2**.

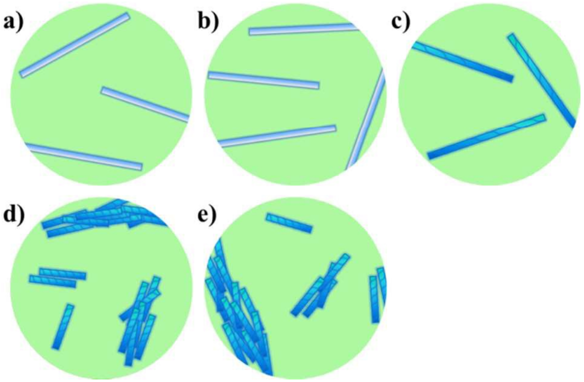

Figure 4. Schematic model for the observed behaviour of nanotubes consisting of achiral **1** and chiral **2** (with DOPC in a ratio of 1:1 amphiphile:DOPC) as a function of the amount of **2**. a) Pure **1**; long, isolated achiral nanotubes. b) < 25% **2**; long, isolated achiral nanotubes. c) 25–50% **2**; long, isolated chiral nanotubes. d) > 50% **2**; short, bundled chiral nanotubes. e) Pure **2**; short, bundled chiral nanotubes.

View Article Online
DOI: 10.1039/C6SC02935C

Cryo-TEM showed that the mixed nanotubes are micrometres long (Figure 2) until **2** becomes the major component (> 50%) and it was hypothesised that mixtures of the amphiphiles containing less than 50% of **2** lead to the formation of long, chiral nanotubes (Figure 4c), which causes a sharp increase in CD signal after exceeding a threshold of 20% of **2** (Figure 3d). In the long nanotubes, the CD signal is more pronounced than in the short nanotubes.[26] Apparently, the long nanotubes (larger aggregated structures) have a higher preference for the absorption of light of a particular handedness, compared to the shorter nanotubes, which leads to a maximum value for the CD signal at 35% of **2**. At higher fractions of chiral **2**, an increase in absorption is observed, signifying the appearance of shorter, bundled tubes and a consequent decrease in CD as in the short nanotubes, the chirality is less pronounced. When **2** is the major component (> 50%) in the mixed tubes, both the UV-vis absorption (Figure 3b) and CD spectra (Figure 3d) become nearly constant, indicating that further increasing the fraction of chiral component **2** in the mixed nanotubes does not result in different self-assembled structures (Figure 4d-e). These results show that chirality is a distinctive factor in controlling the length of individual self-assembled nanotubes, the aggregation of nanotubes and the chirality of the assembly.

The core of amphiphiles **1** and **2** is photoresponsive and can undergo a cyclisation reaction induced by light (see Supporting Information Figure S19 for details) which affects the packing in the nanotubes. We were interested to see if nanotubes of **1**, **2** and mixtures of these compounds can be disassembled by light. In addition, as nanotubes of **2** and mixed nanotubes of **1** and **2**, where the fraction of **2** is higher than 25%, show a significant CD signal, light-triggered disassembly of the chiral nanotubes would provide a way to erase the chiral information with light, offering intriguing possibilities for the development of soft memory devices.[27] We followed the disassembly of the different nanotubes in real time, using widefield fluorescence microscopy and CD spectroscopy, showing the transition from nanotubes to less defined, larger aggregates (Figure 5). As expected, long nanotubes were observed for samples of pure **1** (with DOPC 1:1, Figure 5a), while the shorter nanotubes of pure **2** (with DOPC 1:1, Figure 5c) showed large clusters of nanotubes in accordance with observations by cryo-TEM (Figure 2b). Irradiation *in situ* leads to the deformation, and ultimately disassembly, of the isolated nanotubes of pure **1** (Figure 5b). Nanotube aggregates of pure **2** change morphology under the same conditions as well (Figure 5d), although visualisation of this process is complicated by their size and the resolution of the microscope. For the concomitant CD measurements (Figure 5e), nanotube samples containing 35% and 55% of **2** were diluted and irradiated with low intensity UV light (λ_{irr} = 265 nm, 8 W, see Supporting Information). Note that the light intensity of the widefield microscopy setup is much higher, and the wavelength different, than that of the low intensity UV lamp, causing faster disassembly (Figure 5a–d compared to Figure 5e, further details in the Supporting Information). Both long and short chiral nanotubes show a lag period for disassembly of 2 min under the given conditions. We hypothesise that upon initial irradiation, few molecules are cyclised and disassembly of the nanotubes initiates after a certain threshold of photochemically cyclised amphiphile is reached. After the lag period, initial disassembly is relatively fast and slows down in time. After approximately 2–3 h, the samples are CD silent, the chiral information in the system erased due to disassembly of the tubes.

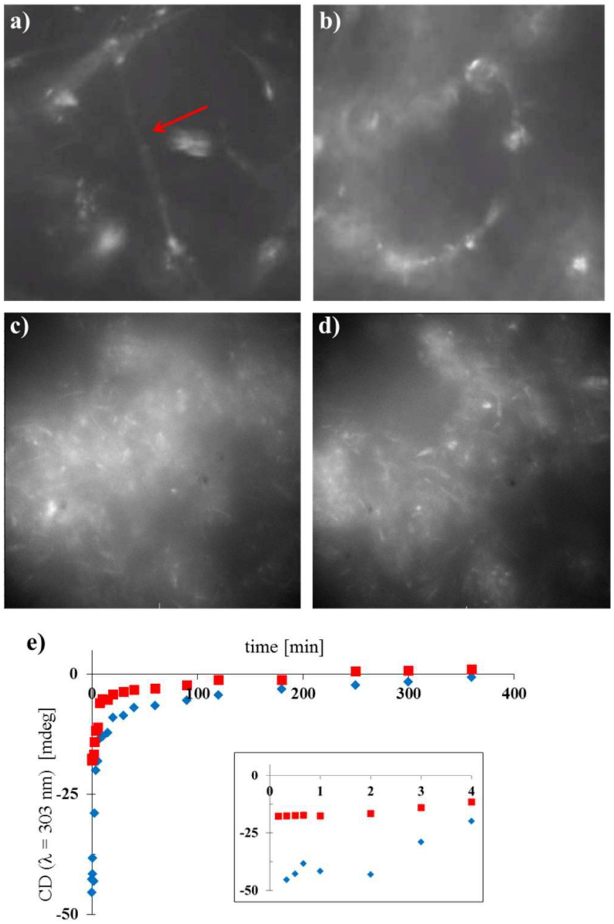

Figure 5. Photochemical disassembly of self-assembled nanotubes in water followed in time by widefield fluorescence microscopy (a–d) and CD spectroscopy (e). a) Image of pure **1** with DOPC (1:1) before irradiation. Isolated nanotube indicated with a red arrow. b) As in (a) after irradiation (t = 53 s, λ_{irr} = 390 nm). c) Image of pure **2** with DOPC (1:1) before irradiation. d) As in (c) after irradiation (t = 53 s, λ_{irr} = 390 nm). e) Low intensity irradiation (λ_{irr} = 265 nm, 8 W) of long chiral nanotubes (**1**:**2**:DOPC 0.65:0.35:1, blue diamonds, $1.6{\cdot}10^{-4}$ M) and short chiral nanotubes (**1**:**2**:DOPC 0.45:0.55:1, red squares, $1.6{\cdot}10^{-4}$ M); inset is an expansion of t = 0–4 min.

Conclusions

In summary, the design, synthesis and study of nanotube-forming light-responsive amphiphiles in which chirality can be used as a means to control the morphology of self-assembled structures is presented. To the best of our knowledge, this

View Article Online
DOI: 10.1039/C6SC02935C

comprises the first example of such nano-objects where the point chirality (stereogenic centre) is present in the hydrophobic part of the amphiphiles, much like in natural membranes. We hypothesise that the hydrophobic volume of the chiral amphiphile **2** is increased, compared to that of the achiral amphiphile **1**, due to the two methyl moieties in C2 of the hydrophobic tails. The increase in hydrophobic volume distorts the long range packing of amphiphile **2**, unlike in other systems, however, the formation of nanotubes is not inhibited by the presence of the methyl moieties in the hydrophobic chains and rather causes the formation of shorter nanotubes.

Three distinct types of assemblies, namely (1) long, isolated achiral, (2) long, isolated chiral and (3) short, bundled chiral nanotubes, can be obtained and they were analysed with various spectroscopic and microscopic techniques. The ratio of chiral to achiral amphiphile provides a reliable handle to control the dimensions of the self-assembled nanotubes and, importantly, the chirality of the molecular constituent can be amplified to the aggregates as a whole. The fact that the nanotubes are in water and that chirality, present in the hydrophobic part of the amphiphilic building blocks, is employed to control the morphology of the self-assembled nanotubes, takes the control over complexity of supramolecular systems one step further. In addition, the nanotubes can be disassembled with light and this responsive feature offers another control element toward smart materials.

Acknowledgements

We thank W. A. Velema and Dr. W. Szymański for insightful comments and useful discussions. This work was supported by the European Research Council (Advanced Investigator grant 227897; BLF), the Ministry of Education, Culture and Science of the Netherlands (Gravitation program 024.001.035, BLF and WRB) and NanoNextNL of the Government of the Netherlands and 130 partners.

Notes and references

1 J. M. Berg, J. L. Tymoczko, and L. Stryer, Biochemistry, W.H. Freeman & Co., New York, USA, 2011

2 R. F. Service, *Science* 2005, **309**, 95.

3 (a) G. Verma and P A. Hassan, *Phys. Chem. Chem. Phys.* 2013, **15**, 17016; (b) Y.-Z. Zhao, L.-N. Du, C.-T. Lu, Y.-G. Jin and S.-P. Ge, *Int. J. Nanomedicine* 2013, **8**, 1621; For reviews see: (c) B. Zheng, F. Wang, S. Dong and F. Huang, *Chem. Soc. Rev.* 2012, **41**, 1621; (d) P. C. Ray, S. A. Khan, A. K. Singh, D. Senapati and Z. Fan, *Chem. Soc. Rev.* 2012, **41**, 3193.

4 (a) L. Brunsveld, B. J. B. Folmer, E. W. Meijer, R. P. Sijbesma, *Chem. Rev.* 2001, **101**, 4071; (b) T. Aida, E. W. Meijer, S. I. Stupp, *Science* 2012, **335**, 813; (c) F. J. M. Hoeben, P. Jonkheijm, E. W. Meijer, A. P. H. J. Schenning, *Chem. Rev.* 2005, **105**, 1491; (d) E. Yashima, K. Maeda, Y. Furusho, Acc. *Chem. Res*. 2008, **41**, 1166; (e) E. Yashima, K. Maeda, H. Iida, Y. Furusho, K. Nagai, *Chem. Rev.* 2009, **109**, 6102.

5 (a) D. G. Blackmond, *Proc. Natl. Acad. Sci. U. S. A.* 2004, **101**, 5732; For reviews see: (b) J. E. Hein and D. G. Blackmond, *Acc. Chem. Res.* 2012, **45**, 2045; (c) K. Soai, T. Kawasaki and T. Shibata, in Catalytic Asymmetric Synthesis, John Wiley & Sons, Inc., Hoboken, N.J, USA, 2010, pp. 891–930.

6 (a) F. Helmich, M. M. Smulders, C. C. Lee, A. P. H. J. Schenning and E. W. Meijer, *J. Am. Chem. Soc.* 2011, **133**, 12238; (b) F. García, P. M. Viruela, E. Matesanz, E. Ortí and L. Sánchez, *Chem. – Eur. J.* 2011, **17**, 7755; (c) A. L. Nussbaumer, D. Studer, V. L. Malinovskii and R. Häner, *Angew. Chem. Int. Ed.* 2011, **50**, 5490; (d) D. Ogata, T. Shikata and K. Hanabusa, *J. Phys. Chem. B* 2004, **108**, 15503; (e) F. García and L. Sanchez, *J. Am. Chem. Soc.* 2012, **134**, 734; (f) S. J. George, Ž. Tomović, M. M. J. Smulders, T. F. A. de Greef, P. E. L. G. Leclère, E. W. Meijer and A. P. H. J. Schenning, *Angew. Chem. Int. Ed.* 2007, **46**, 8206.

7 (a) A. Ajayaghosh, R. Varghese, S. J. George and C. Vijayakumar, *Angew. Chem. Int. Ed.* 2006, **45**, 1141; (b) D. J. van Dijken, J. M. Beierle, M. C. A. Stuart, W. Szymański, W. R. Browne and B. L. Feringa, *Angew. Chem. Int. Ed.* 2014, **53**, 5073; (c) J. J. D. de Jong, L. N. Lucas, R. M. Kellogg, J. H. van Esch and B. L. Feringa, *Science* 2004, **304**, 278.

8 (a) T. W. Anderson, J. K. Sanders and G. D. Pantos, *Org. Biomol. Chem.* 2010, **8**, 4274; (b) A. Ajayaghosh, R. Varghese, S. Mahesh and V. K. Praveen, *Angew. Chem. Int. Ed.* 2006, **45**, 7729; (c) W. Jin, T. Fukushima, M. Niki, A. Kosaka, N. Ishii and T. Aida, *Proc. Natl. Acad. Sci. U. S. A.* 2005, **102**, 10801.

9 (a) R. Eelkema and B. L. Feringa, *Org. Biomol. Chem.* 2006, **4**, 3729; (b) K. Maeda, Y. Takeyama, K. Sakajiri and E. Yashima, *J. Am. Chem. Soc.* 2004, **126**, 16284; (c) N. P. M. Huck, W. F. Jager, B. de Lange and B. L. Feringa, *Science* 1996, **273**, 1686.

10 (a) F. Vera, R. M. Tejedor, P. Romero, J. Barberá, M. B. Ros, J. L. Serrano and T. Sierra, *Angew. Chem. Int. Ed.* 2007, **46**, 1873; (b) J. Wang, D. Ding, L. Zeng, Q. Cao, Y. He and H. Zhang, *New J. Chem.* 2010, **34**, 1394; (c) T. Ishi-i, M. Crego-Calama, P. Timmerman, D. N. Reinhoudt and S. Shinkai, *J. Am. Chem. Soc.* 2002, **124**, 14631.

11 J. van Gestel, A. R. Palmans, B. Titulaer, J. A. Vekemans and E. W. Meijer, *J. Am. Chem. Soc.* 2005, **127**, 5490.

12 A. R. Palmans, J. A. Vekemans, E. E. Havinga and E. W. Meijer, *Angew. Chem. Int. Ed.* 1997, **36**, 2648.

13 J. K. Hirschberg, L. Brunsveld, A. Ramzi, J. A. Vekemans, R. P. Sijbesma and E. W. Meijer, *Nature* 2000, **407**, 167.

14 M. M. Smulders, A. P. H. J. Schenning and E. W. Meijer, *J. Am. Chem. Soc.* 2008, **130**, 606.

15 M. M. Green, M. P. Reidy, R. D. Johnson, G. Darling, D. J. O'Leary and G. Willson, *J. Am. Chem. Soc.* 1989, **111**, 6452.

16 See for example: (a) A. de Jong, E. Casas Arce, T.-Y. Cheng, R. P. van Summeren, B. L. Feringa, V. Dudkin, D. Crich, I. Matsunaga, A. J. Minnaard and D. Branch Moody, *Chem. Biol.* 2007, **14**, 1232; (b) C. Ferrer, P. Fodran, S. Barroso, R. Gibson, E. C. Hopmans, J. Sinninghe Damsté, S. Schouten and A. J. Minnaard, *Org. Biomol. Chem.* 2013, **11**, 2482; (c) P. L.-G. Chong, *Chem. Phys. Lipids*, 2010, **163**, 253; See for general overview and further examples: (d) Molecular Biology of the Cell; B. Alberts, A. Johnson, J. Lewis, M. Raff, K. Roberts and P. Walter; Garland Science: New York, USA, 2002; (e) Biochemistry (Chapters 12 and 13); J. M. Berg, J. L. Tymoczko and L. Stryer; W. H. Freeman: New York, USA, 2002.

17 L. Brunsveld, A. P. H. J. Schenning, M. A. C. Broeren, H. M. Janssen, J. Vekemans and E. W. Meijer, *Chem. Lett.* 2000, **29**, 292.

18 A. C. Coleman, J. M. Beierle, M. C. A. Stuart, B. Maciá, G. Caroli, J. T. Mika, D. J. van Dijken, J. Chen, W. R. Browne and B. L. Feringa, *Nat. Nanotechnol.* 2011, **6**, 547.

View Article Online
DOI: 10.1039/C6SC02935C

19 (a) W. R. Browne, M. M. Pollard, B. de Lange, A. Meetsma and B. L. Feringa, *J. Am. Chem. Soc.* 2006, **128**, 12412; (b) A. C. Coleman, J. Areephong, J. Vicario, A. Meetsma, W. R. Browne and B. L. Feringa, *Angew. Chem. Int. Ed.* 2010, **49**, 6580.

20 C. Hermann, C. Giammasi, A. Geyer and M. E. Maier, *Tetrahedron* 2001, **57**, 8999.

21 T. Sumiyoshi, K. Nishimura, M. Nakano, T. Handa, Y. Miwa and K. Tomioka, *J. Am. Chem. Soc.* 2003, **125**, 12137.

22 T. Wakabayashi, K. Mori and S. Kobayashi, *J. Am. Chem. Soc.* 2001, **123**, 1372.

23 P. A. Levene and L. A. Mikeska, *J. Biol. Chem.* 1929, **84**, 571.

24 M. I. Viseu, A. S. Tatikolov, R. F. Correia and S. M. B. Costa, *J. Photochem. Photobiol. Chem.* 2014, **280**, 54.

25 A. Mammana, A. D'Urso, R. Lauceri and R. Purrello, *J. Am. Chem. Soc.* 2007, **129**, 8062.

26 (a) A. Eisfeld, R. Kniprath and J. S. Briggs, *J. Chem. Phys.* 2007, **126**, 104904; (b) D.-H. Chin, R. W. Woody, C. A. Rohl and R. L. Baldwin, *Proc. Natl. Acad. Sci. U. S. A.* 2002, **99**, 15416.

27 For reviews see: (a) M. Irie, *Chem. Rev.* 2000, **100**, 1685; (b) M. Irie, T. Fukaminato, K. Matsuda and S. Kobatake, *Chem. Rev.* 2014, **114**, 12174.; (c) Molecular Switches; Feringa, B. L., Browne, W. R., Eds.; John Wiley & Sons: Weinheim, Germany, 2011.